

GENUINELY MULTIDIMENSIONAL NON-DISSIPATIVE FINITE VOLUME SCHEMES FOR TRANSPORT

BRUNO DESPRÉS*, FRÉDÉRIC LAGOUTIÈRE**

*Commissariat à l'Énergie Atomique, Bruyères-le-Châtel. despres@cmpax.polytechnique.fr
e-mail: despres@cmpax.polytechnique.fr

**Université Paris-VII and Laboratoire Jacques-Louis Lions, UMR 7598, 175, rue du Chevaleret, 75013 Paris
e-mail: lagoutie@math.jussieu.fr

Keywords: multidimensional transport, finite volume schemes, anti-dissipative schemes, triangular grids.

Abstract

We develop a new multidimensional finite volume algorithm for transport equations. This algorithm is both stable and non-dissipative. It is based on a reconstruction of the discrete solution inside each cell, at every time step. The proposed reconstruction, genuinely multidimensional, allows to recover sharp profiles both in the direction of the transport velocity and in the transverse direction. It is an extension of the one-dimensional reconstructions analyzed in Lagoutière 2007 and Lagoutière 2007.

1 Introduction

The present study¹ concerns reconstruction schemes for transport equations. We are especially interested in schemes that are not dissipative, in particular for initial conditions with discontinuities. This leads to consider reconstructions that are not smooth, on the contrary to usual reconstructions. We indeed develop a discontinuous reconstruction scheme which consists in reconstructing the constant-in-cell datum as a discontinuous (inside each cell) function.

Typically, the goal is to develop transport schemes for mass or volume fractions in multi-fluids. These fractions can be discontinuous (at interfaces between components) or continuous (in mixing zones). A former algorithm was already developed in Després and Lagoutière 2007. It was based in dimension 1 on the *limited downwind scheme* (equivalent to the Ultra-bee limiter for advection with constant velocity) and the multidimensional algorithms were obtained *via* an alternate direction splitting strategy. Results are satisfying, in particular for inter-

faces (see results for interface instabilities in dimensions 2 and 3 in the cited reference). The main drawback of this method is precisely the dimensional splitting, which prevents the algorithm from being used on non-Cartesian grids.

We here present a way to generalize the limited downwind scheme to the case of a general triangular grid. It is based on the geometrical approach followed in Lagoutière 2007, Lagoutière 2007, that provided a new interpretation of the limited downwind algorithm, in terms of reconstruction scheme.

The paper is organized as follows. Sections 2 and 3 present the mathematical and numerical problems and the notations. Then, we recall the reconstruction procedure leading to the limited downwind scheme in dimension 1 (section 4). In section 5, the main subject of the paper is addressed: the extension to upper dimensions of the preceding procedure. The presentation deals with dimension 2. Finally, section 6 exhibits numerical results.

For the time-being, the most efficient algorithms for pure transport rest upon interface reconstruction: see for example SLIC and Youngs' method, Noh and Woodward 1976 and Youngs 1984, and the method of Mosso (Mosso and Cleancy 1995) which is a recent promising enhancement. These methods are essentially limited to Cartesian grids. We here try to derive a truly multidimensional reconstruction algorithm.

¹This work was partially supported by CEA/DIF Bruyères-le-Châtel

2 Model problem

The considered model is the linear transport equation with constant (given) velocity

$$\begin{cases} \partial_t u(t, x) + \operatorname{div}(\mathbf{a}u)(t, x) \\ = \partial_t u(t, x) + \mathbf{a} \cdot \nabla_x u(t, x) = 0 & \text{for } t > 0, \\ u(0, \cdot) = u^0 \in L^\infty(\mathbb{R}^2), \end{cases} \quad (1)$$

where \mathbf{a} is a smooth divergence-free velocity field: $\operatorname{div}(\mathbf{a}) = 0$ for every $(t, x) \in \mathbb{R}^+ \times \mathbb{R}^2$.

The main issue for the numerical treatment of this PDE problem is the *numerical diffusion*. This phenomenon, easily understandable in dimension 1, is much more complex in higher dimension. It shall be decomposed in two different types of diffusion. The diffusion of the first type, which will be called *longitudinal diffusion*, is the one that occurs in the direction of the velocity. It is the diffusion which is present in one-dimensional classical algorithms. The second type diffusion, *transverse diffusion*, is typically multidimensional and is due to the fact that the mesh may not be aligned with the velocity. This distinction between phenomena could appear arbitrary, but is in accordance with the numerical tests. It is illustrated on FIG. 2 and 3 representing numerical solutions obtained with the classical upwind scheme on a square mesh, with, as initial condition, the characteristic function of a square (FIG. 1). The transport velocity is $\mathbf{a} = (1, 0)$ (aligned with the mesh) for FIG. 2 and $\mathbf{a} = (1, 1)$ (diagonal, not aligned with the mesh) for FIG. 3 and the boundary condition on $[0, 1]^2$ are periodic. The results are displayed for time $t = 1$ (after one period).

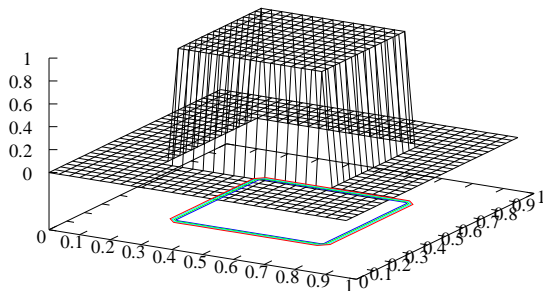


Figure 1. Initial condition.

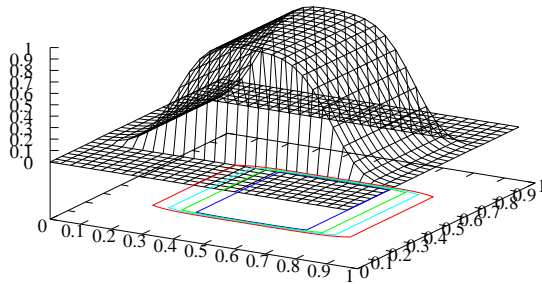


Figure 2. Upwind scheme. $\mathbf{a} = (1, 0)$, aligned with the mesh. Time $t = 1$. The longitudinal diffusion applies in the direction of transport. There is no transverse diffusion.

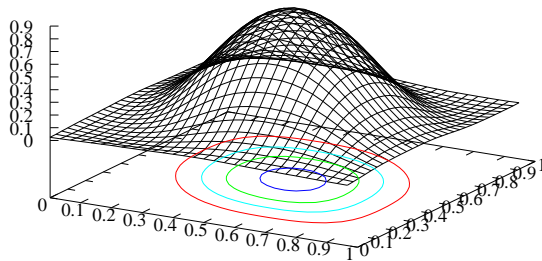


Figure 3. Upwind scheme. $\mathbf{a} = (1, 1)$, not aligned with the mesh. Time $t = 1$. The diffusion which applies orthogonally to the transport direction is brought to light.

The difference between longitudinal and transverse diffusions appears clearly in Després and Lagoutière 2001 which was a previous attempt to elaborate non-dissipative schemes on non-Cartesian grids. Based on mono-dimensional techniques, the schemes derived from this work were longitudinally anti-dissipative, but not transversely.

The new method here described is based on an interpretation of the (anti-dissipative) limited downwind scheme which was proposed in Lagoutière 2007 (previous works are Després and Lagoutière 2002 and Després and Lagoutière 2007). This paper shows that the limited downwind scheme (in dimension 1) can be understood as a reconstruction scheme, decomposed in 3 stages at each time step:

- a reconstruction stage which, starting from a constant-in-cell datum, constructs a new datum, presenting in each cell one discontinuity that separates two constant values,
- a transport stage that solves the transport operation with the new datum,
- a projection stage that computes the mean value of the transported datum in each cell

(see section 4 for precision on the reconstruction stage).

The natural extension to the multidimensional transport problem consists in reconstructing the datum in two steps: in a first step, performing a transverse reconstruction, and performing a longitudinal reconstruction in a second step. This is the technique which is proposed in this work. The following describes precisely these two operations.

3 General numerical formalism

It is the one of finite volume methods for problem (1). We consider a mesh of \mathbb{R}^2 composed of non-empty open triangles $(T_j)_{j \in \mathbb{Z}}$ such that $\bigcup_{j \in \mathbb{Z}} \overline{T_j} = \mathbb{R}^2$ and $T_i \cap T_j = \emptyset$ for every i , every $j \neq i$. For each cell T_j (for $j \in \mathbb{Z}$), one denotes $K(j)$ the set of indices of neighboring cells of T_j (that is to say cells having a common edge with T_j),

$$K(j) = \{k \in \mathbb{Z} \setminus \{j\} \text{ s.t. } \text{meas}_1(\overline{T_j} \cap \overline{T_k}) > 0\}$$

where meas_1 denotes the Lebesgue measure in dimension 1. For $j \in \mathbb{Z}$ and for $k \in K(j)$ (T_j and T_k have an edge in common), one denotes $l_{j,k}$ the length of the common edge,

$$l_{j,k} = \text{meas}_1(\overline{T_j} \cap \overline{T_k})$$

and $\mathbf{n}_{j,k}$ the unit normal vector to the common edge outward to T_j . We thus have $l_{j,k} = l_{k,j}$ and $\mathbf{n}_{j,k} = -\mathbf{n}_{k,j}$ for every $j \in \mathbb{Z}$ and every $k \in K(j)$. We then denote by $K^+(j)$ the set of indices of the downwind neighbors of T_j and by $K^-(j)$ the set of indices of the upwind neighbors of T_j :

$$K^+(j) = \{k \in K(j) \text{ s.t. } \langle \mathbf{a}, \mathbf{n}_{j,k} \rangle > 0\},$$

$$K^-(j) = \{k \in K(j) \text{ s.t. } \langle \mathbf{a}, \mathbf{n}_{j,k} \rangle < 0\}.$$

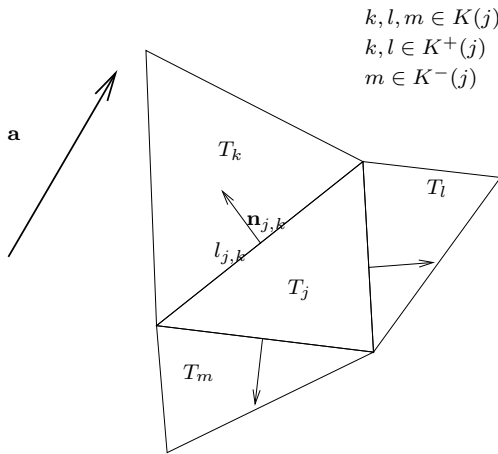


Figure 4. Mesh and notations

Let s_j denote the surface of cell T_j :

$$s_j = \text{meas}_2(T_j)$$

where meas_2 denotes the Lebesgue measure in dimension 2. The general form of the here considered schemes is obtained by choosing a time step $\Delta t > 0$ and by integrating the transport equation of (1) on $[n\Delta t, (n+1)\Delta t] \times T_j$:

$$\frac{u_j^{n+1} - u_j^n}{\Delta t} + \frac{1}{s_j} \left(\sum_{K^+(j)} l_{j,k}(\mathbf{a}_{j,k}^n, \mathbf{n}_{j,k}) u_{j,k}^n + \sum_{K^-(j)} l_{j,k}(\mathbf{a}_{j,k}^n, \mathbf{n}_{j,k}) u_{j,k}^n \right) = 0. \quad (2)$$

In this formula, the quantities $\mathbf{a}_{j,k}^n$ are approximate values of the given velocity $\mathbf{a}(t, x)$ on the edges and the $u_{j,k}^n$ are approximate values of the solution on the edges between times $n\Delta t$ and $(n+1)\Delta t$. The upwind scheme is obtained taking $u_{j,k}^n = u_j^n$ for $k \in K^+(j)$ and $u_{j,k}^n = u_k^n$ for $k \in K^-(j)$. We will propose another definition of these numerical fluxes, intended to provide more precise numerical results.

4 Discontinuous reconstructions in dimension 1

In the following, for every $a, b \in \mathbb{R}$, $\langle a, b \rangle$ denotes the interval $[a, b]$ if $a \leq b$ and the interval $[b, a]$ else, that is to say that we adopt the convention

$$\langle a, b \rangle = [\min(a, b), \max(a, b)]$$

and one has $\langle a, b \rangle = \langle b, a \rangle$.

We here recall the principle of discontinuous reconstruction schemes in dimension 1. Details and proofs lie in Lagoutière 2007 and Lagoutière 2007. We consider a mesh (on \mathbb{R}) with constant space step $\Delta x > 0$ whose cells are the intervals $T_j = ((j-1/2)\Delta x, (j+1/2)\Delta x)$ for $j \in \mathbb{Z}$. It is shown in Lagoutière 2007 that for the transport equation

$$\partial_t u + a \partial_x u = 0,$$

the limited downwind scheme out of Després and Lagoutière 2002 is equivalent to the 3-stages following scheme. Let $(u_j^n)_{j \in \mathbb{Z}}$ be a discrete datum (associated with a constant-in-cell function).

- 1 “Reconstruct” in each cell the discrete datum in a form with more detail (not constant) following the algorithm detailed above.
- 2 Perform the (exact) transport of this reconstructed datum at velocity a for a time Δt .

We now have to assign to each of the sub-cells a value of the reconstructed solution. The adopted principle is quite similar to the one in dimension 1, except that the locus of the discontinuity is determined by the geometrical aspect and not the local values of the datum: it is the line parallel to \mathbf{a} defined just above. The aim is to define a value $u_{j,k}^n$ in the cell $T_{j,k}$ and a value $u_{j,l}^n$ in the cell $T_{j,l}$ by maximizing $|u_{j,l}^n - u_{j,k}^n|$ (to guarantee the anti-dissipativity) and making certain that $s_{j,k}u_{j,k}^n + s_{j,l}u_{j,l}^n = s_j u_j^n$ (to guarantee the conservativity). On the other side, following the same rules as in dimension 1, we impose that the triplet $\{u_l^n, u_{j,l}^n, u_{j,k}^n\}$ has the same monotony as the pair $\{u_l^n, u_j^n\}$ and that the triplet $\{u_{j,l}^n, u_{j,k}^n, u_k^n\}$ has the same monotony as the pair $\{u_j^n, u_k^n\}$. These constraints imply in particular that the datum in T_j would not be reconstructed if u_j^n was a local extremum in the transverse direction. The algorithm is

- if $u_j^n \notin (u_k^n, u_l^n)$ (if u_j^n is a local extremum in the transverse direction), we do not reconstruct \bar{u} in the cell T_j (that is to say, $u_{j,l}^n = u_{j,k}^n = u_j^n$),

- if $u_j^n \in (u_k^n, u_l^n)$,

– if $(s_j u_j^n - s_{j,l} u_l^n) / s_{j,k} \in [u_j^n, u_k^n]$, we define

$$\begin{cases} u_{j,l}^n = u_l^n, \\ u_{j,k}^n = (s_j u_j^n - s_{j,l} u_l^n) / s_{j,k}; \end{cases}$$

– if $(s_j u_j^n - s_{j,k} u_k^n) / s_{j,l} \in [u_j^n, u_l^n]$, we define

$$\begin{cases} u_{j,l}^n = (s_j u_j^n - s_{j,k} u_k^n) / s_{j,l}, \\ u_{j,k}^n = u_k^n. \end{cases}$$

Lemma 1. *The Courant-Friedrichs-Lewy (CFL) condition on the time step is not degraded by the transverse reconstruction.*

Proof. *The standard condition for the upwind scheme for the cell T_j is*

$$\Delta t \frac{\sum_{k \in K^+(j)} l_{j,k}(\mathbf{a}, n_{j,k})}{s_j} \leq 1,$$

i.e., in the particular studied case,

$$\Delta t \frac{l_{j,k}(\mathbf{a}, n_{j,k}) + l_{j,l}(\mathbf{a}, n_{j,l})}{s_j} \leq 1. \quad (4)$$

The CFL condition for sub-cells $T_{j,k}$ and $T_{j,l}$ are

$$\Delta t \frac{l_{j,k}(\mathbf{a}, n_{j,k})}{s_{j,k}} \leq 1 \quad \text{and} \quad \Delta t \frac{l_{j,l}(\mathbf{a}, n_{j,l})}{s_{j,l}} \leq 1. \quad (5)$$

Let us denote l_j the length of the segment separating $T_{j,k}$ and $T_{j,l}$:

$$l_j = \text{mes}_1(\overline{T_{j,k}} \cap \overline{T_{j,l}}).$$

One has

$$s_{j,k} = \frac{l_j \times l_{j,k}(\mathbf{a}, n_{j,k})}{2} \quad \text{and} \quad s_{j,l} = \frac{l_j \times l_{j,l}(\mathbf{a}, n_{j,l})}{2},$$

and

$$s_j = s_{j,k} + s_{j,l} = \frac{l_j \times (l_{j,k}(\mathbf{a}, n_{j,k}) + l_{j,l}(\mathbf{a}, n_{j,l}))}{2}$$

The two inequalities of (5) and inequality (4) thus rewrite

$$\frac{2\Delta t}{l_j} \leq 1,$$

they are equivalent.

Remark 1. *Once the solution is reconstructed, the transport of it is related to one-dimensional transport since $T_{j,l}$ and $T_{j,k}$ have only one upwind and one downwind neighbor: respectively, T_m, T_l and T_m, T_k . When T_j has only one downwind neighbor, we do not perform the transverse reconstruction and can consider the problem as mono-dimensional, performing (virtually) the cutting but assigning the value u_j^n to each sub-cell.*

After this transverse reconstruction, the algorithm is more classical, lying on the fact that the transport is mono-dimensional, as noticed in remark 1. We thus can use the algorithm of our own choice. In the following, we pitch on the limited downwind one. This can also be understood as a second reconstruction, longitudinal.

6 Numerical results

We present a few results obtained with the algorithm described herein. Different velocity fields are used: translation and rotation fields.

For all the test-cases, the spatial domain is $[0, 1]^2$. The triangular mesh has been generated by the software FreeFem++: see FIG. 7.

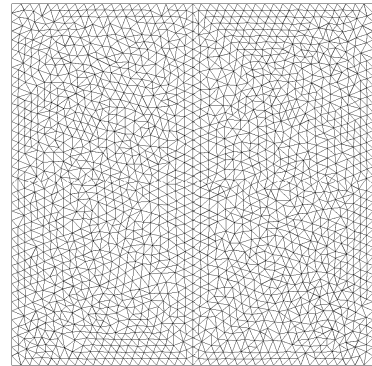


Figure 7. Example of FreeFem++ mesh, used for the numerical tests (here, 3766 triangles).

For all the test-cases, the Courant number $\max_{j \in \mathbb{Z}} \Delta t \frac{\sum_{k \in K^+(j)} l_{j,k}(\mathbf{a}, n_{j,k})}{s_j}$ takes the value 0.1.

6.1 Translation field

“translation of a square” Here we consider the velocity

$$\mathbf{a}(t, x, y) = \begin{pmatrix} 1 \\ 1 \end{pmatrix}.$$

This first test is the translation of the characteristic function of a square,

$$u^0(x, y) = \chi_{[0.3, 0.7]^2}(x, y).$$

The boundary conditions are periodic in x and y . Initial condition and results at time $t = 1$ (after one revolution) are reported in FIG. 8 and FIG. 9 reports the result by the upwind scheme.

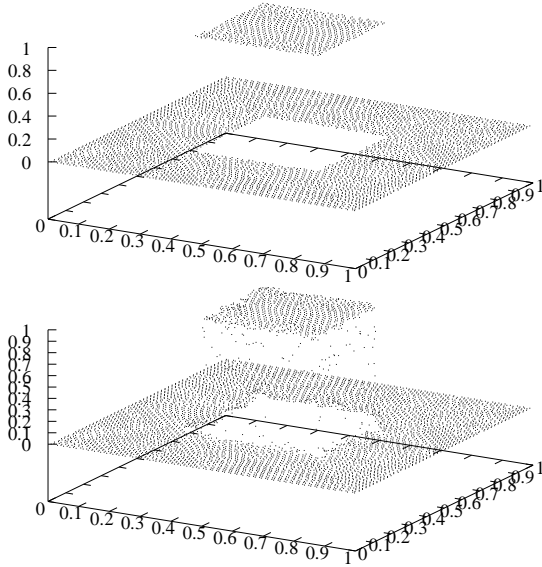


Figure 8. Translation of a square with 5874 cells.

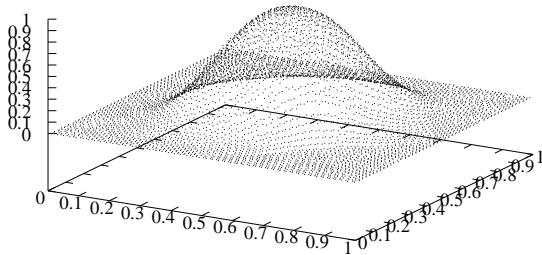


Figure 9. Translation of a square with 5874 cells, upwind scheme.

6.2 Rotation field

“Rotation of a square” The velocity field is here

$$\mathbf{a}(t, x, y) = \begin{pmatrix} 2\pi y \\ -2\pi x \end{pmatrix}$$

and the initial condition is the same as in the preceding test. The final time is $t = 1$. Figure 10 presents the result.

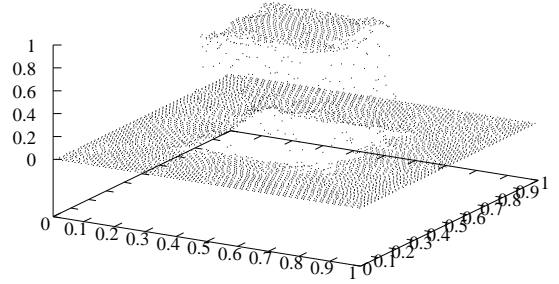


Figure 10. Rotation of a square with 5874 cells.

Zalesak’s test-case The velocity field is the same as in the preceding test,

$$\mathbf{a}(t, x, y) = \begin{pmatrix} 2\pi y \\ -2\pi x \end{pmatrix}$$

and the initial condition is taken from the original paper Zalesak 1979:

$$u^0(x, y) = \chi_Z(x, y)$$

where

$$Z = C \setminus R$$

with

$$C = \{(x, y); (x - 0.5)^2 + (y - 0.75)^2 \leq 0.0225\},$$

$$D = \{(x, y); |x - 0.5| \leq 1/40 \text{ and } y \leq 17/20\}.$$

Initial condition and result computed with 5874 cells at time $t = 1$ lie in FIG. 11. Then, FIG. 12 represents the same for a mesh made of 23618 cells, and FIG. 13 for a mesh composed of 94472 cells.

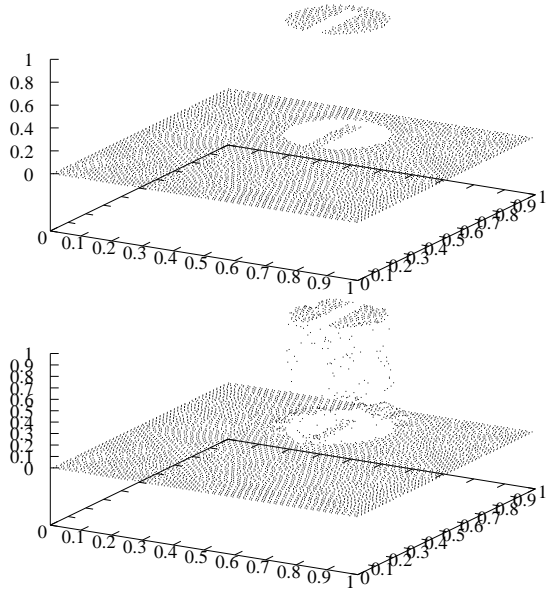


Figure 11. Zalesak's test-case with 5874 cells.

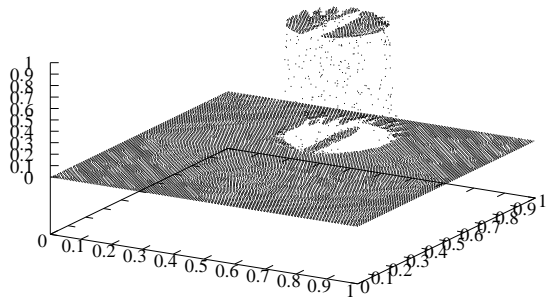


Figure 12. Zalesak's test-case with 23618 cells.

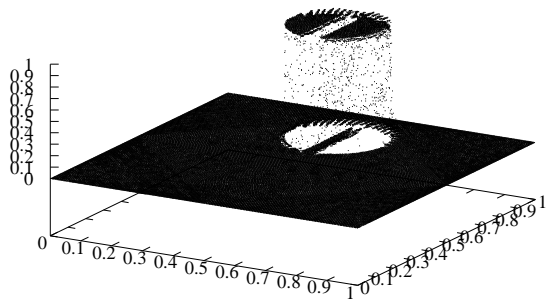


Figure 13. Zalesak's test-case with 94472 cells.

“Deformation of a rectangle” The velocity field is now not constant in time:

$$\mathbf{a} = \text{sgn}(1 - t) \begin{pmatrix} 3\pi(y - 0.5)^2 \\ -3\pi(x - 0.5)^2 \end{pmatrix},$$

which means that at time $t = 1$ the field is reversed. The initial condition is the characteristic function of a rectangle:

$$u^0(x, y) = \chi_{[0.2, 0.7] \times [0.45, 0.55]}(x, y).$$

The exact solution at time 2 coincides with the initial condition.

We observe the initial condition (FIG. 14) and the results at time $t = 1$ (FIG. 15) with 5874 cells and finally the result at time $t = 2$ with 5874 cells (FIG. 16), 23618 cells (FIG. 17) and 94472 cells (FIG. 18). The result given by the upwind scheme with 94472 cells is reported on FIG. 19.

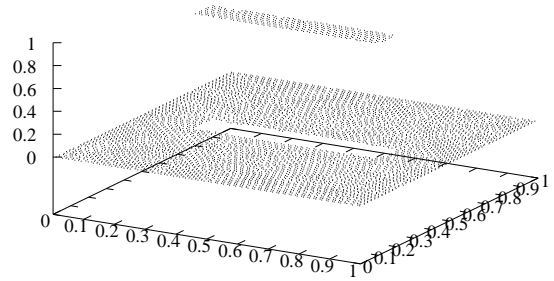


Figure 14. Initial condition with 5874 cells.

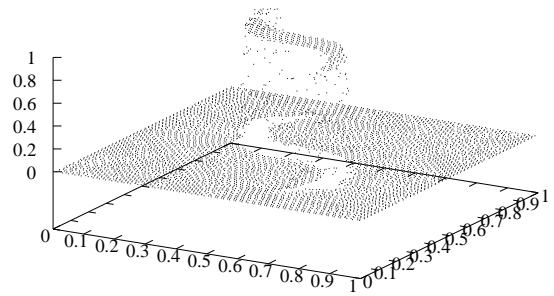


Figure 15. Numerical solution with 5874 cells at time $t = 1$.

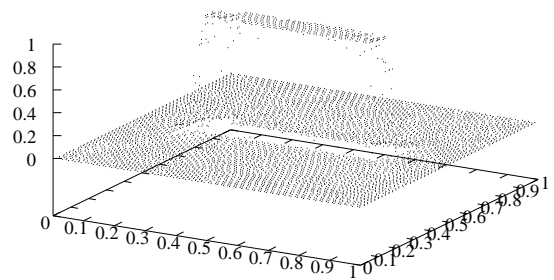


Figure 16. Numerical solution with 5874 cells at time $t = 2$.

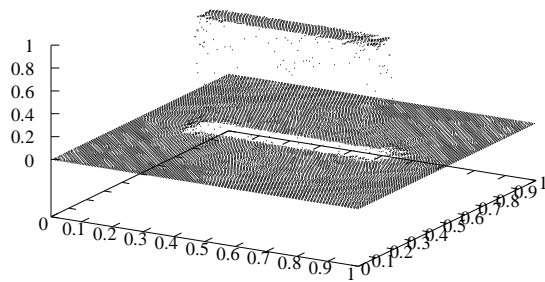


Figure 17. Numerical solution with 23618 cells at time $t = 2$.

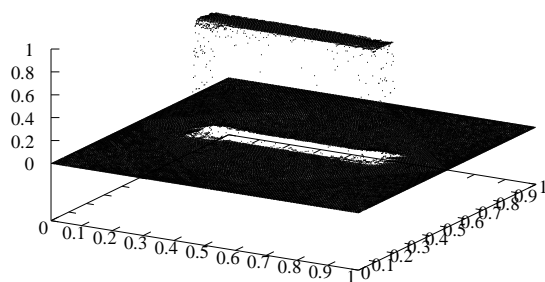


Figure 18. Numerical solution with 94492 cells at time $t = 2$.

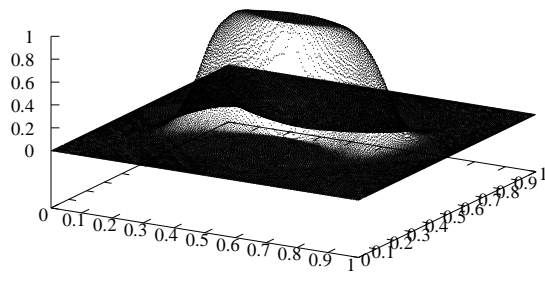


Figure 19. Numerical solution with 94492 cells at time $t = 2$ with the upwind scheme.

7 Final comments

We developed a new method for the numerical transport in dimension 2. The approach is truly multidimensional in the sense that it does not reduce to a mono-dimensional reconstruction of interfaces. The numerical results show the anti-dissipative behavior of the algorithm. The results are nevertheless not perfect. Indeed, the discontinuity lines may be degraded in long time (see FIG. 11, 12, 13).

Next study will concern the extension on general meshes (non-triangular) and in dimension 3, and the application to gas dynamics equations.

References

- Després B. and Lagoutière F. (2001): *Generalized Harten formalism and longitudinal variation diminishing schemes for linear advection on arbitrary grids*. M2AN Math. Model. Numer. Anal. 35, no. 6, pp. 1159–1183.
- Després B. and Lagoutière F. (2002): *Contact discontinuity capturing schemes for linear advection and compressible gas dynamics*. J. Sci. Comput., 16 (2001), no. 4: pp. 479–524.
- Després B., Lagoutière F. (2007): *Numerical resolution of a two-component compressible fluid model with interfaces*, to appear in Progress in Computational Fluid Dynamics.
- Lagoutière F. (2007): *Stability of reconstruction schemes for scalar hyperbolic conservation laws*, in revision.
- Lagoutière F. (2007): *Non-dissipative reconstruction schemes satisfying entropy inequalities*, in revision.
- Mosso S. and Cleancy S. (1995): *A geometrical derived priority system for Young's interface reconstruction*. LA-CP-95-0081, LANL report.
- Noh W. F. and Woodward P. R. (1976): *SLIC (Simple Line Interface Calculation)*. Springer Lecture Notes in Physics, 25: pp. 330–339.
- D. L. Youngs, An interface tracking method for a 3D eulerian hydrodynamics code, Technical Report 44/92/35, AWRE (1984).
- Zalesak S. T. (1979): *Fully multidimensional flux-corrected transport algorithms for fluids*, Journal of Computational Physics, 31, pp. 335–362.